Proceedings of FEDSM2006
2006 ASME Joint U.S. - European Fluids Engineering Summer Meeting
July 17-20, Miami, FL, USA

FEDSM2006-98536

INTERFACE-TRACKING SIMULATION OF TWO-PHASE FLOWS BY PHASE-FIELD METHOD

Naoki TAKADA
National Institute of Advanced Industrial Science and Technology (AIST)
16-1, Onogawa, Tsukuba, Ibaraki 305-8569, Japan
Tel: +81-29-861-8232, Fax: +81-29-861-8722,
E-mail: naoki-takada@aist.go.jp

Akio TOMIYAMA
Graduate School of Science and Technology,
Kobe University
1-1, Rokkodai, Nada, Kobe, Hyogo 657-8501, Japan
E-mail: tomiyama@mech.kobe-u.ac.jp

ABSTRACT

The purpose of this study is to examine multi-physics computational fluid dynamics method, NS-PFM, which is a combination of Navier-Stokes (NS) equations with phase-field model (PFM) based on the free-energy theory, for interface-capturing/tracking simulation of two-phase flows. First, a new NS-PFM which we have proposed was applied to immiscible, incompressible, isothermal two-phase flow problems with a high density ratio equivalent to that of an air-water system. In this method, a Cahn-Hilliard equation was used for prediction of diffusive interface configuration. The numerical simulations demonstrated that (1) predicted collapse of two-dimensional liquid column in a gas under gravity agreed well with available data at aspect ratios of column = 1 and 2, and (2) coalescence of free-fall drops into a liquid film was successfully simulated in three dimensions. Second, we took heat transfer into account in another NS-PFM which solves a full set of NS equations and the van-der-Waals equation of state. Through a numerical simulation of a non-ideal fluid flow in the vicinity of the critical point, it was confirmed that the NS-PFM is applicable to thermal liquid-vapor flow problems with phase change.

INTRODUCTION

In recent years, phase-field model (PFM) [1] has grown popular as one of useful tools for well understanding complex phenomena involving self organization of mesoscopic structures in multi-component systems, such as two-phase flows [1,2,3], solidification of binary alloys [4] and formation of polymer membranes [5]. Based on the van-der-Waals, Cahn-Hilliard free-energy theory [6], PFM describes an interface as a volumetric transition zone with a finite width between pure components (phases), across which physical properties vary steeply but continuously. The coexistence of two phases with the diffusive interface is allowed by a free-energy functional which has a double-well potential of an order parameter (mass density or molar concentration) and depends on square of its local gradient, without imposing topological constraints on interface as phase boundary. In the theory, surface tension is defined as an excessive free energy per unit area caused by local gradient of the order parameter inside the interface zone, enabling calculation of the continuous body force without using interfacial curvature and normal vector. As a result, the PFM-based method for two-phase flows does not necessarily require conventional elaborating algorithms for advection and reconstruction of interface [7,8] and continuum surface force modeling [9] in front-tracking, level-set and volume-of-fluid (VOF) methods [10-12]. This feature simplifies interface-tracking calculation on a fixed spatial grid. The PFM method therefore has attractive advantages over the other methods, easy implementations of multi-dimensional advection of interface and associated heat and mass transfer across the interface [1-3].

PFM methods are categorized into two types; a direct numerical method using Navier-Stokes (NS) equations (NS-PFM) [3,4], and a lattice Boltzmann method (LBM) [13,14] using mesoscopic kinetic equations for the velocity distribution of a number density of fictitious fluid particles [15-18]. Both types had been applied only to two-phase flows with a small density difference because of numerical instability. To overcome the difficulty, two kinds of two-phase LBM proposed by Chen et al. [19] and Inamuro et al. [20] adopted conventional finite difference scheme for problems with contact discontinuity and solution algorithm for Poisson equation of pressure, respectively. Based on the latter LBM [20], we have recently proposed a NS-PFM [21,22] applicable to two-phase flow problems at a high density ratio. One of advantages of NS-PFM over two-phase LBM is to save computational memory, because the number of macroscopic variables in NS equations is generally less than that of mesoscopic variables (particle-velocity distribution functions) in the LBM kinetic equations.

The purpose of this study is to examine the basic interface-capturing/tracking capability of two kinds of NS-PFM for numerical simulation of two-phase flows with a high density

ratio or with phase change. First, a NS-PFM we have proposed [21,22] is applied to immiscible, incompressible, isothermal two-phase flows with the same density ratio as that of an air-water system. In order to verify the method, the numerical results are compared with available data in other experimental and numerical studies. Second, we took heat transfer into account in another NS-PFM [21] using a full set of NS equations and the van-der-Waals equation of state, for a direct numerical simulation of compressible thermal non-ideal fluid flow with phase change in the vicinity of the critical point.

NOMENCLATURE

A	long-range interaction of van-der-Waals fluid particles
a	width of liquid column
B	short-range interaction of van-der-Waals fluid particles
c	specific heat
$\mathbf{g}$	gravitational acceleration vector
H	height of liquid column or position of drop in z direction
$\mathbf{I}$	second-rank isotropic tensor
k	thermal conductivity
n^2	aspect ratio of liquid column (=H/a)
$\mathbf{P}$	pressure tensor including surface-tension effect
P'	pressure including excess free energy of interface
p	pressure in homogeneous fluid
T	parameter of free-energy function (and/or temperature)
t	time
$\mathbf{u}$	flow velocity vector
x,y,z	position in Cartesian coordinate system

Greek letters

Δt	time step width
Γ	mobility of index function ϕ in Cahn-Hilliard equation
ϕ	index function to indicate interface profile
η	chemical potential
κ_S	surface tension parameter
κ_ϕ	interface thickness parameter
μ	viscosity of fluid
ρ	mass density of fluid
σ	surface tension
$\boldsymbol{\tau}$	viscous stress tensor

Subscript

G	gas phase
L	liquid phase

Superscript

*	dimensionless parameter

BASIS OF PHASE-FIELD METHOD (NS-PFM)

Isothermal two-phase fluids with a high density ratio

The numerical method NS-PFM proposed for immiscible, incompressible, isothermal two-phase flows [21,22] solves a set of a continuity equation, momentum conservation equations, and a Cahn-Hilliard advection-diffusion equation describing time evolution of the interface profile [1,2,6,20],

$$\nabla\cdot\mathbf{u}=0, \tag{1}$$

$$\frac{D\mathbf{u}}{Dt}=\frac{1}{\rho}\left[-\nabla\cdot\mathbf{P}+\nabla\cdot\boldsymbol{\tau}\right], \tag{2}$$

$$\frac{\partial\phi}{\partial t}+\nabla\cdot(\phi\mathbf{u})=-\nabla\cdot\left[-\Gamma\phi\nabla\eta\right]. \tag{3}$$

In Eq.(3), the continuous scalar variable ϕ is an index (so-called order parameter [1-6]) to describe interface profile [20] which is continuously distributed in the whole flow field. In this study, the chemical potential η is derived from a free-energy functional Ψ with the van-der-Waals bulk energy [15,18,20] and an excessive energy caused by gradient of ϕ [1] as follows,

$$\eta\equiv\frac{\delta\Psi}{\delta\phi}=T\ln\left(\frac{\phi}{1-B\phi}\right)-2A\phi+\frac{T}{1-B\phi}-\kappa_\phi\nabla^2\phi, \tag{4}$$

where κ_ϕ is a parameter to control interfacial thickness at $T<8A/(27B)$. For simplicity, the mobility Γ is set to be constant.

The density ρ is given as a continuous function of ϕ [20],

$$\rho=\frac{\rho_L+\rho_G}{2}+\frac{\rho_L-\rho_G}{2}\sin\left(\frac{(\phi_L+\phi_G)/2-\phi}{|\phi_L-\phi_G|}\pi\right), \tag{5}$$

where ϕ_G and ϕ_L are arbitrary thresholds on ϕ to distinguish the gas and liquid phases. The pressure tensor $\mathbf{P}$ is expressed as [1],

$$\mathbf{P}=\left(p-\kappa_S\rho\nabla^2\rho-\frac{\kappa_S}{2}|\nabla\rho|^2\right)\mathbf{I}+\kappa_S\nabla\rho\otimes\nabla\rho, \tag{6}$$

where κ_S denotes the strength of surface tension σ, and p is the pressure in homogeneous field. Calculating $\mathbf{P}$, the right-hand-side first term of Eq.(6) is replaced with $(P'-\kappa_S|\nabla\rho|^2)\mathbf{I}$ just for computational convenience [20-22]. The parameter κ_S constant in the whole flow field is determined from the definition of σ as an excessive free energy on a flat interface [1,3,15-20],

$$\sigma\equiv\kappa_S\int_{-\infty}^{+\infty}|\nabla\rho|^2\,dx, \tag{7}$$

where x is the axis along the normal direction of the interface. The viscous stress $\boldsymbol{\tau}$ in Eq.(2) has a coefficient μ for Newtonian fluid, which is given by a linear interpolation on ρ [20].

$$\mu=\mu_G+\frac{\mu_L-\mu_G}{\rho_L-\rho_G}(\rho-\rho_G) \tag{8}$$

In this NS-PFM, the following numerical techniques were adopted for solving the above equations [21,22]. Scalar and vector variables were located in staggered arrangement on a fixed regular grid with unit cells. The solenoidal velocity $\mathbf{u}$ and the effective pressure $P'=P+\kappa_S|\nabla\rho|^2$ [20] were calculated using the projection algorithm [25]. The advection term in Eq.(2) was calculated with a 3rd-order upwind finite difference scheme [26], while that in Eq.(3) was calculated with a 4th-order central difference scheme (CDS). Gradients of scalar variables were calculated with a 4th-order CDS, while a 2nd-order CDS was applied to the viscous term. Time marching was based on the 2nd-order Runge-Kutta's scheme with a constant Δt.

Thermal two-phase flow with phase change

Another NS-PFM for simulating thermal two-phase flows with phase change adopts a full set of NS equations for a non-ideal fluid and the van-der-Waals equation of state [1,3,18,21]. In this study, they are solved by using the MacCormack scheme. Time evolution of total energy E of the fluid is described in conservative form by the following equation [1,3],

$$\frac{\partial E}{\partial t}+\nabla\cdot(E\mathbf{u})=\nabla\cdot\left[(-\mathbf{P}+\boldsymbol{\tau})\cdot\mathbf{u}+k\nabla T-\kappa_S\rho(\nabla\cdot\mathbf{u})\nabla\rho\right], \tag{9}$$

$$E=\frac{1}{2}\rho\mathbf{u}^2+\rho(cT-A\rho)+\frac{\kappa_S}{2}|\nabla\rho|^2, \tag{10}$$

where the pressure p of $\mathbf{P}$ is expressed as follows [15,18,19].

$$p=\rho T(1-B\rho)^{-1}-A\rho^2 \tag{11}$$

NUMECAL RESULTS OF TWO-PHASE FLOW

This section describes numerical results of three kinds of two-phase flow obtained with NS-PFM. All of the simulations were carried out on a fixed spatial grid with uniform mesh width $\Delta x=\Delta y=\Delta z=1.0$ in Cartesian coordinate system. As for incompressible two-phase flow, density and viscosity ratios ρ_L/ρ_G and μ_L/μ_G were set at 801.7 and 73.76 respectively, which correspond to those of air-water system at 1 atm. and at room temperature. The other parameters were set as follows; $A=B=1$, $T=0.293$, $\kappa_\phi=0.1$, and $\phi_G=0.3802$, $\phi_L=0.2751$, $|\mathbf{g}|=2\times10^{-3}$, $\Gamma=12$, $\rho_L=1$, $\rho_G=1.247\times10^{-3}$, and $\Delta t=0.0125$.

Collapse of 2D liquid column in a gas under gravity

The NS-PFM [21,22] was applied to collapse of two-dimensional liquid column in a gas under gravity **g** in a rectangular domain surrounded with non-slip solid walls (Fig.1), for examining the interface-capturing and -tracking capabilities in comparison with available data [12,23,24].

First, the simulation was conducted at an aspect ratio of column $n^2= H/a=2$. In both cases of spatial resolution, Case1 and Case2 (Table1), initial column width a was assumed to be equivalent to 146mm in air-water system. The effect of gravity on the fluid was taken into account only in the regions at $\rho>\rho_G$. Shapes of the liquid column at dimensionless times $t^*= nt(|\mathbf{g}|/a)^{0.5}=1.159$, 2.318, and 3.477 in each of Case1 and Case2 are shown in Fig.2 (a) and (b) respectively, where the solid lines inside gradation-colored diffusive interface zone are drawn at three contour values of density $\rho=\rho_M=(\rho_G+\rho_L)$ and $\rho_M\pm(\rho_L-\rho_G)/4$. The dimensionless times correspond to 0.1, 0.2, and 0.3 seconds respectively, for water column with width a=146mm in air [24]. The interfacial shapes in both low and high resolutions, Case1 and Case2, agree well with each other at each time t^*. From the density contour lines drawn with a certain distance at each t^* in both the cases, it is confirmed that the interface retained its initial finite thickness sufficiently during collapse. In Fig.3, cross-sectional profile of ρ along x axis on the bottom wall surface at each time is drawn as solid line in each case of resolutions. As shown by the time series of the lines in each of the figures (a) and (b), while the interface moved on the wall surface from left side to right side, the initial profile also was retained sufficiently without numerical oscillation and diffusion until t^*=2.90 in both Case1 and Case2.

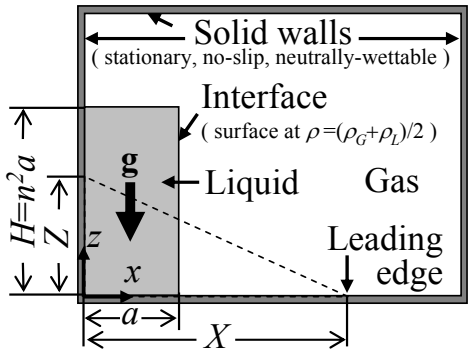

Fig.1 Schematic of 2D computational domain.

Table 1 Parameters in simulation of collapse of liquid column

Case#	Aspect ratio $n^2=H/a$	Width of column a		Surface tension σ	Viscosities	
		PFM ($\Delta x=1$)	air&water (m)		μ_G(gas)	μ_L(liquid)
1	2	10Δx	1.46×10^{-1}	7.11×10^{-5}	1.43×10^{-7}	1.06×10^{-5}
2		18Δx		2.30×10^{-4}	3.47×10^{-7}	2.56×10^{-5}
3	1	40Δx	5.72×10^{-2}	7.42×10^{-3}	4.96×10^{-6}	3.46×10^{-4}
4		80Δx	1.14×10^{-1}			
5	2	20Δx	2.86×10^{-2}			
6		40Δx	5.72×10^{-2}			

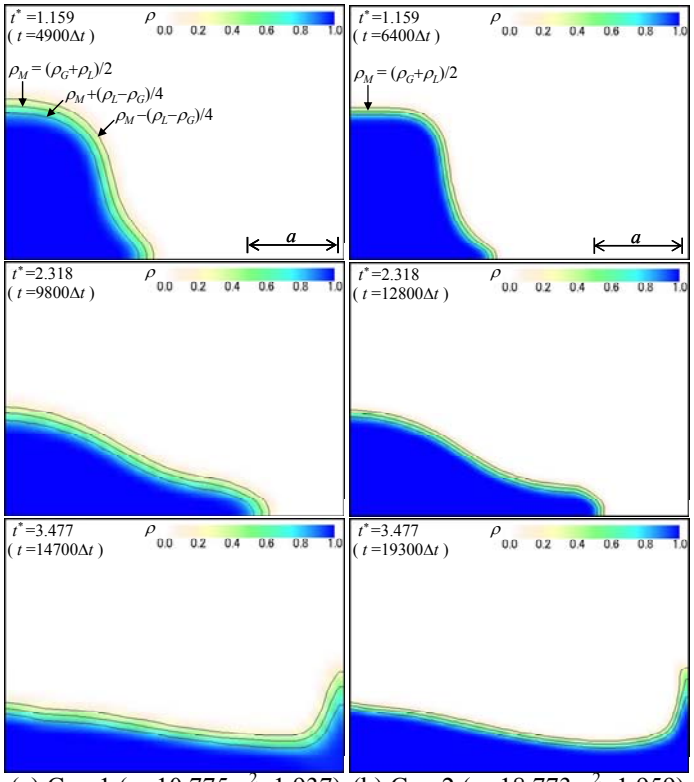

(a) Case1 (a=10.775,n^2=1.937) (b) Case2 (a=18.773,n^2=1.959)

Fig.2 Snapshots of diffuse-interfacial profile in collapse of liquid column with initial width a and aspect ratio n^2=2 under gravity **g** at time $t^*=nt(|\mathbf{g}|/a)^{0.5}$ (Δt= 0.0125).

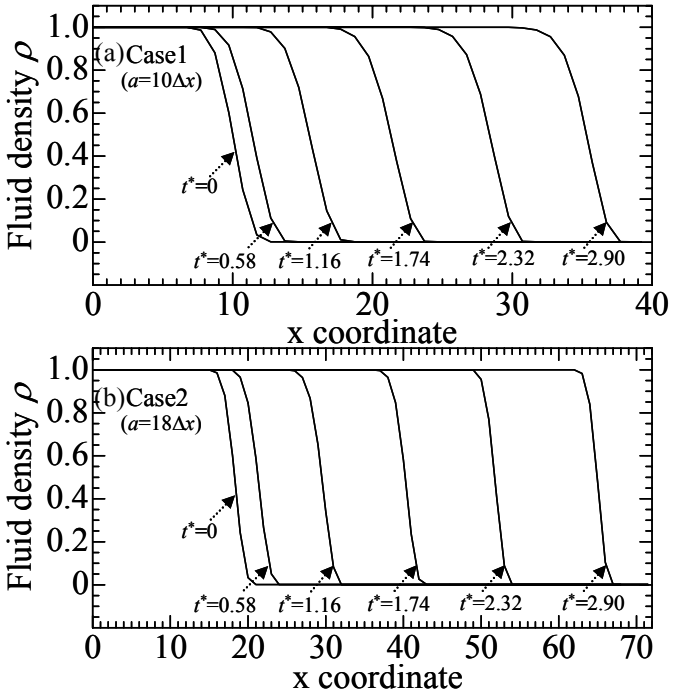

Fig.3 Time series of profile of density ρ across gas-liquid interface on a bottom solid wall at time $t^*=nt(|\mathbf{g}|/a)^{0.5}$.

Hereafter, the numerical results are compared with experimental results in actual air-water system and other numerical solutions obtained with VOF and MPS methods [12,23,24]. Figure 4 show time series of dimensionless horizontal leading-edge position $X^*=X/a$ of the column on a surface of bottom solid wall. In measurement of X, the diffusive interface with a finite thickness was represented by a contour surface at $\rho=\rho_M$. In the figure, solid and broken lines denote the present results in low and high resolutions of Case1 and Case2 respectively, while symbols denote the experimental results [23,24] in air-water system and the numerical solutions given by VOF and MPS methods [12,24], respectively. The result of X^* obtained with the NS-PFM at both resolutions agreed with the other predictions [12,23,24] until dimensionless time $t^*=3.0$. As shown in Figs.2 and 3, the interface in the NS-PFM has a finite thickness caused by the free-energy increase which is proportional to squared gradient of ϕ, $\kappa_\phi|\nabla\phi|^2/2$ in Eq.(6) [1,6]. The leading edge of column therefore tends to become more rounded, compared with those in conventional numerical methods which describe an interface as phase boundary with no volume. That is the reason why the result of the leading-edge position in this study deviated gradually from

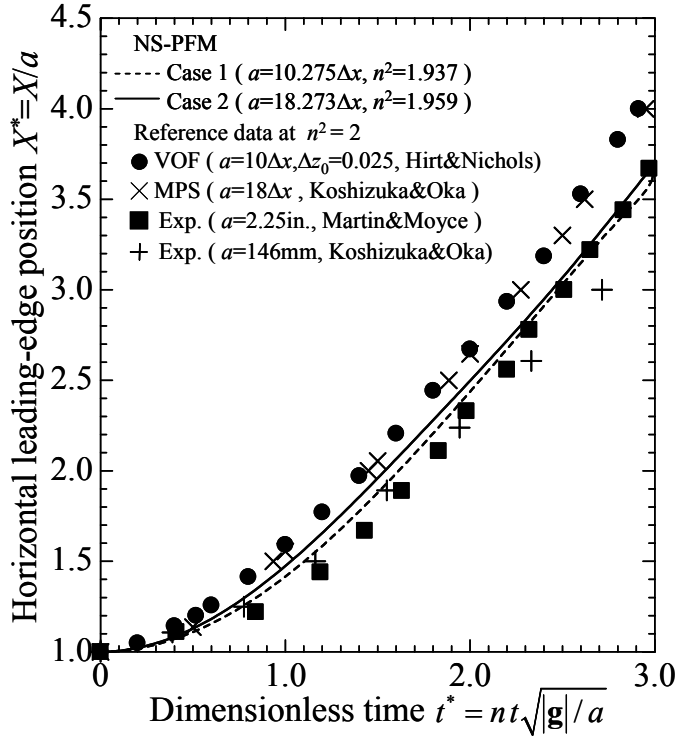

Fig.4 Time series of dimensionless leading-edge position $X^*=X/a$ of 2D liquid column with initial width a and aspect ratio $n^2=H/a=2$.

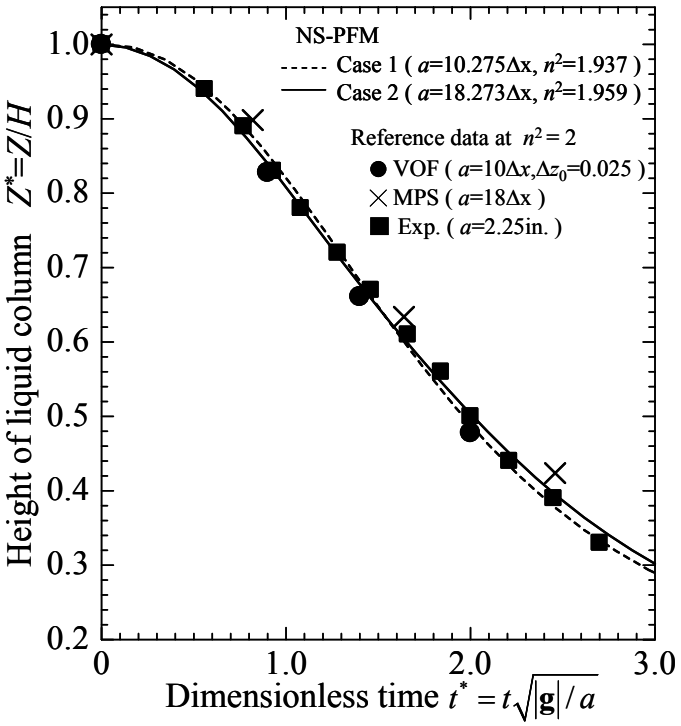

Fig.5 Time series of dimensionless height $Z^*=Z/H$ of 2D liquid column with initial width a and aspect ratio $n^2=2$.

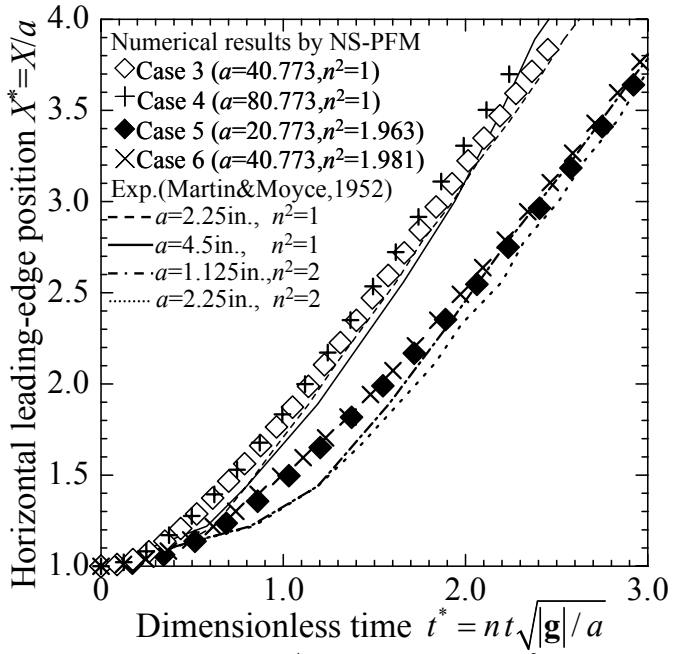

Fig.6 Time series of $X^*=X/a$ at aspect ratio $n^2=1$ and 2.

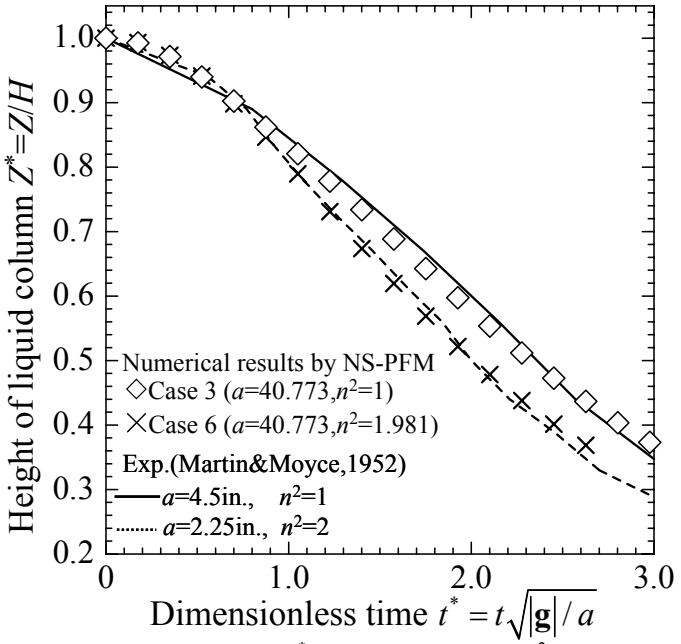

Fig.7 Time series of $Z^*=Z/H$ at aspect ratio $n^2=1$ and 2.

those obtained with VOF and MPS methods as the liquid column collapsed. To the contrary, dimensionless height of the column $Z^*=Z/H$ in each case of resolutions was predicted in better agreement with those obtained with VOF and MPS methods [12,24] as well as the experimental data [23,24] until dimensionless time $t^*=t(|\mathbf{g}|/a)^{0.5}=3.0$, as shown in Fig.5. In other cases at aspect ratio $n^2=1$ and 2, Case3-Case6 (Table1), there were also good agreements between the numerical predictions by the NS-PFM (denoted by symbols in Figs.6 and 7) and the experimental data (lines) [23] in terms of both X^* and Z^*.

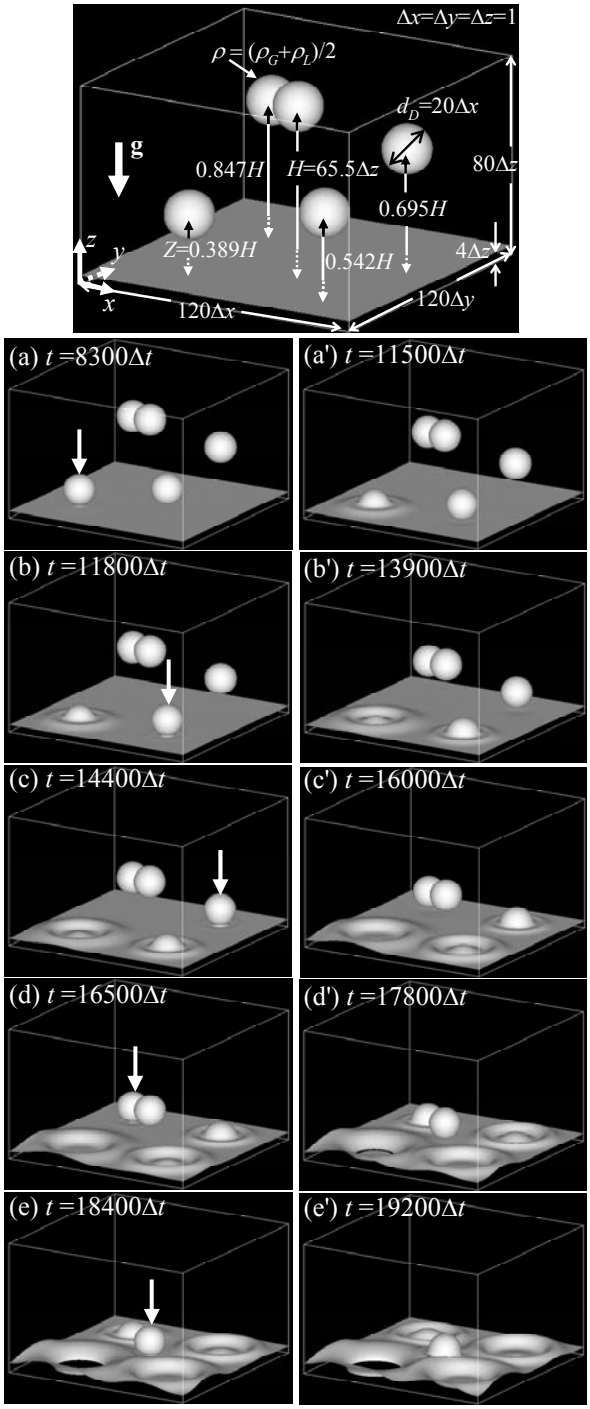

Fig.8 Initial condition (top-row figure) and time series of snapshot of free-fall drops and liquid film just at contact of each drop (pointed by white arrow in left column) and their half merge (right column), where $\Delta t=0.0125$.

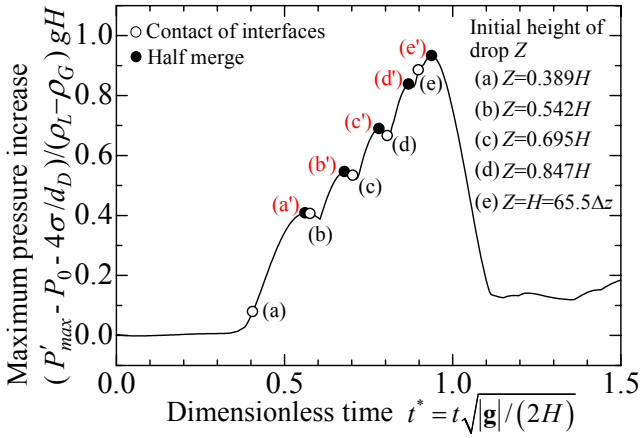

Fig.9 Time series of maximum pressure in coalescence of liquid film and free-fall drops with diameter $d_D=20\Delta x$ and initial height Z under gravity $\mathbf{g}$ in a stagnant gas.

Coalescence of 3D drops and liquid film under gravity

As the second example, we simulated coalescence of three-dimensional drops falling through a stagnant gas into a liquid film sustained on a horizontal solid wall under gravity (Fig.8). The diameter of each drop $d_D=20\Delta x$ in the simulation was equivalent to 10mm in actual air-water system. As seen in Figs.8 and 9, pressure built up just at each contact of drops with liquid film ((a)-(e) in order of time, denoted by open circles in Fig.9), and then reached its local maximum values after the drops penetrated by half into the liquid film ((a')-(e'), closed circles). In each coalescence of drops with normalized initial height $Z^*=Z/H=0.389$, 0.542, 0.695, 0.847, and 1.0, the maximum pressure increase was approximately equivalent to initial potential energy of the drop in the same way as Ref.[21].

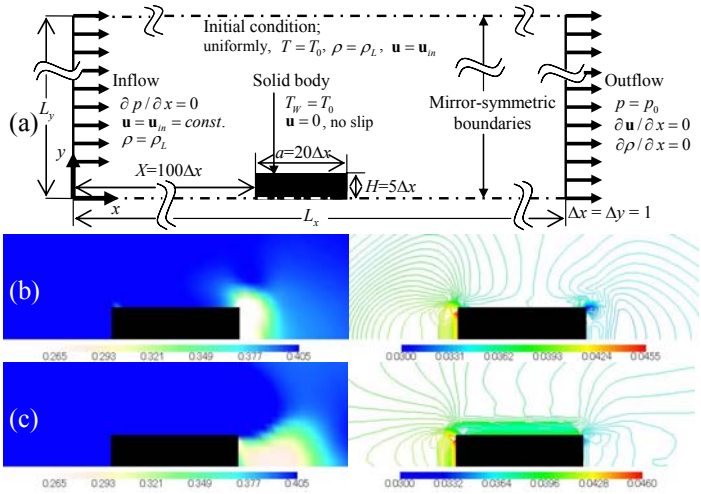

Fig.10 Non-ideal fluid flow around a bluff body. (a)Computational domain, and snapshots of density (left column) and pressure (right) fields at (b)$t=1000\Delta t$ and (c)$10000\Delta t$.

Non-ideal fluid flow with phase change around body

This subsection describes a direct numerical simulation of 2D van-der-Waals fluid flow around a bluff body (Fig.10). The NS-PFM using Eqs.(9)-(11) was applied to a test case with a condition of $A=B=1$, $c=1.5$, $\kappa_S=0.01$, $k=\mu=0.2$, $\mathbf{g}=\mathbf{0}$, $\Delta t=0.05$, and $\mathbf{u}_{in}=(0.05,0)$. The liquid with $\rho_L=0.405$ at temperature $T=T_0=0.293$ in the domain with $L_x=300\Delta x$ and $L_y=50\Delta y$ was surrounded with mirror-symmetric boundaries on the top and

bottom sides, uniform inflow and free outflow at pressure $p=p_0$ =0.0354 on the other sides. A no-slip solid body with constant $T_W=T_0$, width $a=20\Delta x$ and half height $H=5\Delta y$ was located at the bottom. As shown in Fig.10 (b) and (c), a gas with ρ_G =0.265 was generated from the liquid on the back of the body, where p decreased below the initial value p_0 at an equilibrium state.

CONCLUSIONS

In this study, two versions of numerical method, NS-PFM, combining Navier-Stokes (NS) equations with the phase-field model (PFM) [1-3,15-20] based on the free-energy theory [6] were applied to several two-phase flow problems, for examining the basic interface-tracking capability. The first version of NS-PFM we proposed [21,22] computed immiscible, incompressible, isothermal two-phase flows at a high density ratio equivalent to that of air-water system. From the numerical results, it was confirmed that (1) the volume flux driven by a local chemical potential gradient in the Cahn-Hilliard equation [6] plays an important role in self-organizing reconstruction of gas-liquid interface with no numerical diffusion and oscillation, (2) collapse of two-dimensional liquid column in a gas under gravity was predicted in good agreement with well-known experimental and other numerical data [12,23,24], and (3) successive coalescences of liquid drops falling through a stagnant gas into a stagnant liquid film under gravity were simulated successfully in three dimensions. The second version of NS-PFM was used for a direct numerical simulation of two-dimensional thermal non-ideal fluid flow around a bluff solid body in the vicinity of critical point. The DNS demonstrated that the NS-PFM is able to reproduce interface motions in liquid-vapor flows with phase change and heat transfer without using conventional interface-capturing/tracking techniques.

REFERENCES

[1] Anderson, D. M., McFadden, G. B., and Wheeler, A. A., 1998, "Diffuse-Interface Methods in Fluid Mechanics," Annu. Rev. Fluid Mech., **30**, pp.139-165.

[2] Jacqmin, D., 1999, "Calculation of Two-Phase Navier-Stokes Flows Using Phase-Field Modeling," J. Comput. Phys., **155**, pp.96-127.

[3] Jamet, D., Lebaique, O., Coutris, N. and Delhaye, J. M., 2001, "The Second Gradient Method for the Direct Numerical Simulation of Liquid-Vapor Flows with Phase Change," J. Comput. Phys., **169**, pp.624-651.

[4] Bi, Z., and Sekerka, R. F., 1998, "Phase-Field Model for Solidification of a Binary Alloy," Physica A, **261**, pp.95-106.

[5] Morita, H., Kawakatsu, T., and Doi, M., 2001, "Dynamic Density Functional Study on the Structure of Thin Polymer Blend Films with a Free Surface," Macromolecules, **34**, pp.8777-8783.

[6] Cahn, J. W., and Hilliard, J. E., 1958, "Free Energy of a Nonuniform System. I. Interfacial Free Energy," J. Chem. Phys., **28**, pp.258-267.

[7] Kunugi, T., and Satake, S., 1999, "Direct Numerical Simulation of Turbulent Free-Surface Flow," Turbulence and Shear Flow Phenomena-1, pp.621-626, Begell House, New York.

[8] Yabe, T., Xiao, F., and Utsumi, T., 2001, "The Constraind Interpolation Profile Method for Multiphase Analysis," J. Comput. Phys., **169**, pp.556-593.

[9] Brackbill, J. U., Kothe, D. B. and Zemach, C., 1992, "A Continuum Method for Modeling Surface Tension," J. Comput. Phys., **100**, pp.335-354.

[10] Tryggvason, G., Bunner, B., Esmaeeli, A., Juric, D., Al-Rawahi, N., Tauber, W., Han, J., Nas, S., and Jan, Y.-J., 2001, "A Front-Tracking Method for the Computations of Multiphase Flow," J. Comput. Phys., **169**, pp.708-759.

[11] Chang, Y. C., Hou, T. Y., Merriman, B., and Osher, S., 1996, "A Level Set Formulation of Eulerian Interface Capturing Methods for Incompressible Fluid Flows," J. Comput. Phys., **124**, pp.449-464.

[12] Hirt, C. W. and Nichols, B. D., 1981, "Volume of Fluid (VOF) Method for the Dynamics of Free Boundaries," J. Comput. Phys., **39**, pp.201-225.

[13] Chen, S. and Doolen, G. D., 1998, "Lattice Boltzmann Method for Fluid Flows," Annu. Rev. Fluid Mech., **30**, pp. 329-364.

[14] Succi, S., 2001, *The Lattice Boltzmann Equation for Fluid Dynamics and Beyond*, Oxford at the Clarendon Press, UK.

[15] Swift, M. R., Orlandini, E., Osborn W. R., and Yeomans, J. M., 1996, "Lattice Bolztammn Simulations of Liquid-Gas and Binary Fluid Systems," Phys. Rev. E, **54**, pp.5041-5052.

[16] Takada, N., Tomiyama, A., and Hosokawa, S., 2003, "Numerical Simulation of Drops in a Shear Flow by a Lattice-Boltzmann Binary Fluid Model," Comput. Fluid Dyn. J., **12** (3), pp.475-481.

[17] Takada, N., Misawa, M., Tomiyama, A. and Hosokawa, S., 2001, J. Nucl. Sci. Technol., **38** (5), pp.330-341.

[18] Seta, T., and Kono, K.., 2004, "Thermal Lattice Boltzmann Method for Liquid-Gas Two-Phase Flows in Two Dimensions," JSME Int. J. B-Fluid T., **47** (3), pp.572-583.

[19] Chen, Y., Teng, S., and Ohashi, H., 1999, "On the Lattice Boltzmann Modeling of Multi-phase Flows," Proc.3rd Organized Multiphase Flow Forum'99, 58-64, Yokohama, Japan.

[20] Inamuro, T., Ogata, T., Tajima, S., and Konishi, N., 2004, "A Lattice Boltzmann Method for Incompressible Two-Phase Flows with Large Density Differences," J. Comput. Phys., **198**, pp.628-644.

[21] Takada, N., Misawa, M., and Tomiyama, A., 2005, "A Phase-Field Method for Interface-Tracking Simulation of Two-Phase Flows," Proc. 2005 ASME Fluids Engineering Division Summer Meeting and Exhibition, Paper No. FEDSM2005-77367, Houston, TX, USA.

[22] Takada, N., and Tomiyama, A., 2006, "A Numerical Method for Two-Phase Flows Based on a Phase-Field Model," JSME Int. J. B-Fluid T., **49** (3), in press.

[23] Martin, J. C., and Moyce, W. J., 1952, "An Experimental Study of the Collapse of Liquid Columns on a Rigid Horizontal Plane," Philos. Trans. Roy. Soc. London, Ser.A, **244**, pp.312-324.

[24] Koshizuka, S., and Oka, Y., 1996, "Moving-Particle Semi-Implicit Method for Fragmentation of Incompressible Fluid," Nucl. Sci. Eng., **123**, pp.421-434.

[25] Chorin, A. J., 1968, "Numerical Solution of the Navier-Stokes Equations," Math. Comput., **22**, pp.745-762.

[26] Kawamura, T., and Kuwahara, K., 1984, "Computation of High Reynolds Number Flow around a Circular Cylinder with Surface Roughness," AIAA Paper, 84-0340.